Available online at www.sciencedirect.com
SCIENCE DIRECT
Carbohydrate Research 341 (2006) 624–633
Carbohydrate RESEARCH

A computational study of structure–reactivity relationships in Na-adduct oligosaccharides in collision-induced dissociation reactions

Kazuhiko Fukui,[a,*] Akihiko Kameyama,[b] Yuri Mukai,[a] Katsutoshi Takahashi,[a] Noriko Ikeda,[c] Yutaka Akiyama[a] and Hisashi Narimatsu[b]

[a]*Computational Biology Research Center (CBRC), National Institute of Advanced Industrial Science and Technology (AIST), 2-41-6 Aomi, Koutou, Tokyo 135-0064, Japan*
[b]*Research Center for Glycoscience (RCG), National Institute of Advanced Industrial Scinece and Technology (AIST), 1-1-1 Umezono, Tsukuba, Ibaraki 305-8566, Japan*
[c]*Fujitsu Laboratories Ltd, Kawasaki, Kanagawa, Japan*

Received 24 November 2005; received in revised form 27 December 2005; accepted 7 January 2006
Available online 26 January 2006

Abstract—Elucidating the fragmentation mechanisms in oligosaccharides using theoretical calculations is useful in analyzing the experimentally obtained mass spectra. Semi-empirical and ab initio quantum mechanics calculations were used to study the relationship between the structure and reactivity and the chemical properties of oligosaccharides. In these calculations, sodium-cationized oligosaccharides were investigated to determine Na^+ ion affinity at several binding positions; in addition, the dependence of the glycosidic bond cleavage on the Na^+ position was examined. The calculated structures reported in this study are directed at interpreting experimentally observed fragment ions, resulting from the cleavage of the glycosidic bonds. The calculated results for oligosaccharides containing between three and five monosaccharide units (27 oligosaccharides) were compared with experimental data generated by matrix-assisted laser-desorption/ionization (MALDI) using a quadrupole ion trap (QIT) with a time-of-flight (TOF) mass spectrometer (MS).

Keywords: Oligosaccharides; Glycosyl bond; Model; Simulation; MALDI-QIT MS

1. Introduction

Glycoprotein oligosaccharides are known to play a vital role in biological processes, including protein conformation, stability, intra and intercellular signaling, and molecular receptor recognition.[1,2] Because the structures of the oligosaccharides in glycoproteins are in many cases related to their biological function, it is important to identify their fine structures, including the complex isomers arising from linkage types, branching, and α-, β-configurations at the anomeric position. Although the inability to identify complex isomers is intrinsic in MS analyses, several examples involving tandem mass spectrometry in which different fragment ions and/or different intensities of the same fragment ions were observed for oligosaccharides with the same sequences but different structures have been reported.[3] Therefore, the high sensitivity and high-throughput analysis of mass spectrometry is expected to be a powerful method in the analysis of oligosaccharides.[3–5]

We have recently reported an approach to a high-throughput analysis of oligosaccharides utilizing an observational tandem mass spectral library.[6–8] This library contains the collision-induced dissociation (CID) spectra of sodium-adduct ions of a large variety of oligosaccharides, which affords the characteristic fragment patterns in CID spectra.[6,8] However, no reports discuss the theoretical aspects of why each oligosaccharide affords the characteristic fragment patterns.

* Corresponding author. Tel.: +81 3 3599 8667; fax: +81 3 3599 8491; e-mail: k-fukui@aist.go.jp

0008-6215/$ - see front matter © 2006 Elsevier Ltd. All rights reserved.
doi:10.1016/j.carres.2006.01.013

One of the keys for this question may lie behind the coordination of metal ions to the oligosaccharide molecules, because the $[M+H]^+$ ions of oligosaccharides afford less characteristic fragment patterns than the $[M+Na]^+$ ions.[9–11] Additionally, the elucidation of the fragmentation mechanisms for oligosaccharides would be useful in interpreting the experimentally obtained CID spectra and in assigning these spectra to the appropriate oligosaccharides. In this context, this study focused on the participation of the sodium ion in the fragmentation of oligosaccharides by comparing molecular models of sodium-cationized complexes with the observational CID spectra in our library.

Semi-empirical methods allow for sufficiently fast calculations of molecules that cannot be modeled conveniently using ab initio methods while still providing information regarding electronic structure. These calculations have been used widely in the study of the conformations of proteins, nucleic acids, and polysaccharides.[12] Some of the semi-empirical methods currently used include the Modified Neglect of Differential Overlap (MNDO), the Austin Model 1 (AM1), and the Parameterized Model 3 and Model 5 (PM3 and PM5). Of these methods, PM5 includes a new parameter set with Li, Be, B, Na, Mg, K, Ca, Zn, Cd, Hg atoms, etc. The average accuracy for the heats of formation over all of the parameterized elements and the algorithms for the PM5 method have been improved by approximately a factor of four compared with the current AM1 and PM3 parameterizations.[13] PM5 has been reported to be suitable for modeling complexes with alkali metals, making it a popular choice for calculations of biological systems involving saccharides and metal ions.[14] In this report, semi-empirical PM5 calculations were performed to study the structure–reactivity relationships for sodium-adduct oligosaccharides that were experimentally analyzed in CID mass spectrometry.

2. Experimental

2.1. MALDI-QIT-TOF Mass spectrometry

Mass measurements were carried out using a matrix-assisted laser-desorption ionization (MALDI) quadrupole ion trap time-of-flight (TOF) mass spectrometer (AXIMA-QIT; Shimadzu). A nitrogen laser (337 nm) was used for the laser-desorption/ionization. A detailed configuration of the AXIMA-QIT is described elsewhere.[25] All oligosaccharides were purchased from one of the following distributors: Glyko (San Leandro, CA), Dextra Laboratories (Reading, UK), or Sigma–Aldrich (St. Louis, MO). The structures of the 27 oligosaccharides containing between three and five monosaccharide units analyzed using the AXIMA-QIT are shown in Figure 1. The samples were analyzed by placing 0.5 μL of analyte (≈2 μM) on the target plate followed by 0.5 μL of a 2,5-dihydroxybenzoic acid (2,5-DHB; Bruker-Daltonik) solution (10 mg/mL in 20% ethanol). The spot was allowed to dry and inserted into the MS for analysis. All collision-induced dissociation (CID) spectra were obtained from Na-adduct ions. The collision energy was adjusted to reduce the intensity of the parent ion to less than 15% of the area of the base peak.[3]

2.2. Calculations

The 27 oligosaccharides shown in Figure 1 were used to computationally analyze the structure–reactivity relationship of the fragmentation in the CID spectra. The initial configurations for all of the models were obtained using SWEET2.[15–17] In SWEET2, the conformations are optimized using a complete molecular mechanics force field (MM3) interfaced with the software package TINKER.[18–20] In this study, the geometries of the neutral oligosaccharides generated by SWEET2 were first optimized using a semi-empirical calculation. Then, the alkali metal cationized complex ions, $[M+Na]^+$, were optimized by placing the Na^+ at the appropriate position of the oligosaccharide for analyzing the affinity ($M+Na^+ \rightarrow [M+Na]^+$) and preferential binding position of Na^+. The semi-empirical PM5 calculations were carried out using the MOPAC 2002 program on a cluster at Fujitsu Laboratories Ltd.[13] The full optimizations of the geometries for the neutral samples and $[M+Na]^+$ complexes were performed at the PM5 level. To compare the semi-empirical PM5 results with those of ab initio calculations, quantum chemical calculations were performed using the Hartree Hock (HF) and density functional theory (DFT) with the Gaussian03 programs on a PC cluster and IBM Regatta at the Computational Biology Research Center (CBRC). The PM5 output data for the neutral and sodiated oligosaccharide ions were used as the input for the quantum calculations, and those models were then optimized using suitable basis sets [HF/6-31G(d), B3LYP/6-31(d), and B3LYP/6-31(d,p)]. All of the optimized geometries were checked to have positive vibrational frequencies by normal mode calculations. In this study, classical trajectory simulations were also performed to analyze the structural stability of the sodiated oligosaccharide ions at a constant temperature. Molecular dynamics (MD) simulations are an invaluable tool in studying structural and dynamic details at the atomic/molecular level, and in linking these details to the experimentally observable properties of molecules.[21] For the empirical potential functions of the MD simulations, the potential parameters obtained from GLYCAM based on the HF/6-31G* ab initio calculations were used.[22,23] The trajectories for the sodiated samples were computed for several energies to investigate the effect of the available energy on the stability

of the Na^+ binding position and associated structures. The energy was controlled by varying the kinetic energy. The MD simulations were conducted at temperatures of 298, 350, 400, and 500 K.

Abbreviation	Structure	Assigned fragment Ions
A-022	Fucα1 – 2Galβ1 – 4GlcNAc	Y_2(100),P(8),P-H_2O(7)
A-023	GalNAcα1 3 / Fucα1 2 > Gal	$Y_{1\alpha}$(100),$Z_{1\beta}$(9),P(9)
A-024	Galα1 3 / Fucα1 2 > Gal	$Y_{1\beta}$(100),P(12),$Y_{1\alpha}$(10),$Z_{1\beta}$(9)
A-025	Galα1 – 3Galβ1 – 4Gal	Y_2(100),B_2(41),Y_1(15),P(8),168.9(6)
A-028	Fucα1 4 / Galβ1 3 > GlcNAc	$Y_{1\beta}$(100)
A-029	Galβ1 4 / Fucα1 3 > GlcNAc	$Y_{1\beta}$(100),$Z_{1\beta}$(23),P(5)
A-030	Galα1 – 3Galβ1 – 4GlcNAc	Y_2(100),550.2(20),B_2(18),P(13),Y_1(11)
A-031	Manα1 6 / Manα1 3 > Man	275.0(100),$Y_{1\beta}$(34),P(11),190.1(8), 160.1(5)
GSL-003	Neu5Acα2 – 3Galβ1 – 4Glc	Y_2(100)
M-012	Neu5Acα2 – 6Galβ1 – 4Glc	Y_2(100),P(24)
S-002	Galβ1 – 4Galβ1 – 4Glc	Y_2(100),4670,B2(17),304.9(10), P-H_2O(10)
S-004	Fucα1 – 2Galβ1 – 4Glc	Y_2(100), P(9)
A-033	Fucα1 4 / Fucα1 – 2Galβ1 3 > GlcNAc	Y2α(100),Z1α(9),Y2α/Y1α(9),P(8)
A-034	Fucα1 – 2Galβ1 4 / Fucα1 3 > GlcNAc	$Y_{2\alpha}$(100),$Y_{2\alpha}$/$Y_{1\beta}$(13),$Z_{1\beta}$(11), P(11),$Y_{1\alpha}$(6)
A-035	Fucα1 4 / Neu5Acα2 – 3Galβ1 3 > GlcNAc	$Y_{2\beta}$(100),P(9)
A-036	Neu5Acα2 – 3Galβ1 4 / Fucα1 3 > GlcNAc	$Y_{2\alpha}$(100)
N-001	Manα1 – 3Manβ1 – 4GlcNAcβ1 – 4GlcNAc	B_3(100),Y_2(26),P(12), P-H_2O(11),B_2(11)
M-001	Galβ1 – 4GlcNAcβ1 – 3Galβ1 – 4Glc	B_2(100), Z_3(24), Y_2(22), C_2(13)
M-002	Galβ1 – 3GlcNAcβ1 – 3Galβ1 – 4Glc	Z_3(100), B_2(87), C_2(50), Y_2(30),C_3(22)
S-003	GalNAcα1 3 / Fucα1 2 > Galβ1 – 4Glc	$Y_{1\alpha}$(100),B_2(64),B_2/$Y_{B\beta}$(54), $C_{1\alpha}$(12)

Figure 1. Schematic representation of oligosaccharides and the experimentally observed MS/MS fragment ions. The nomenclature for the assigned fragment ions is based on that proposed by Domon and Costello.[36] The parentheses show the percentage of the relative abundance (%). The abbreviations used are: Gal, galactose; Man, mannose; Glc, glucose; Fuc, fucose; GlcNAc, *N*-acetylglucosamine; Neu5Ac, *N*-acetylneuraminic acid. All residues are in the pyranose form. P represents the abundance of the parent ion.

Abbreviation	Structure	Assigned fragment Ions
A-038	GlcNAcβ1 – 2Manα1 6 > Man GlcNAcβ1 – 2Manα1 3 > Man	478.4(100),Y_2(88), Y_2/Y_2(19), 275.5(12),$Y_{1\alpha}$(9)
A-039	Manα1 6 > Manα1 6 > Man Manα1 3 > Manα1 3 > Man	599.3(100),$Y_{2\alpha}$(19), P(8)
A-040	GalNAcα1 3 > Galβ1 4 > Gal Fucα1 2 > Fucα1 3 > Gal	$Y_{1\beta}$(100),$B_{2\alpha}/Y_{1\beta}$(10), $B_{2\alpha}$(9),P(6)
A-041	**Galα1 3** > Galβ1 4 > Gal Fucα1 2 > Fucα1 3 > Gal	$Y_{1\beta}$(100), P(8)
M-005	Fucα1 – 2Galβ1 – 3GlcNAcβ1 – 3Galβ1 – 4Glc	Y_4(100),P(24),C_3(15), 387.9(11),B_3(9)
M-006	Fucα1 4 > GlcNAcβ1 – 3Galβ1 – 4Glc Galβ1 3 >	Y_3(100),C_2(45), $B_2/Y_{1\beta}$(32),$Z_{3\alpha}$(25), B_2(19)
M-007	Galβ1 4 > GlcNAcβ1 – 3Galβ1 – 4Glc Fucα1 3 >	$Y_{1\beta}$(100),$B_2/Y_{1\beta}$(32), C_2(23),B_2(20),Y_{1b}(18)

Figure 1. (*continued*)

3. Results and discussion

3.1. CID Spectra of sodium-adduct ions of oligosaccharides

The fragment patterns in the CID spectra of oligosaccharides vary in the species of ions and in their relative intensities according to the structure, particularly in the case of sodium-adduct ions as the parent ions.[5] Figure 2a shows the MS/MS spectrum of S-003 generated by MALDI-QIT-TOF MS. All of the fragment ions derived from $[M+Na]^+$ at *m*/*z* 714.2 were sodium-adduct ions that were assigned in Figure 2b. Because oligosaccharide S-003 has no acidic functionality, the sodium ion should form a positive-charge center in each fragment ion. Although one bond cleavage divides the molecule to two parts, the intensities of the resulting fragment ions are usually not even. For example, while B_2 and $C_1\alpha$ were strong signals, their counterparts, Y_1 (*m*/*z* 203) and $Z_1\alpha$ (*m*/*z* 493), respectively, were very weak signals. This might be due to an uneven distribution of the sodium ion in the S-003 molecule.

It has also been suggested that the metal ion can undergo coordination with several atoms simultaneously, resulting in the stabilization of a glycosidic bond, which generally contains the most basic oxygens in an oligosaccharide.[9] The binding position of sodium might affect the oligosaccharide molecule where the fragmentation is likely to occur. The relative intensities of the signals in the CID spectra, which vary according to the CID energy, give some information regarding the dissociation tendencies of the oligosaccharide molecules. To investigate these tendencies in oligosaccharide S-003, a series of measurements of the dependence of the fragmentation on the CID energy were carried out. As shown in Figure 2c, although the relative intensities of the fragment ions varied according to the CID energy, the order of the intensities remained constant at all of the CID energies examined with the exception of the $B_2/Y_{2\beta}$ double cleavage ion. These results suggested that the order from most to least stable bond in the glycosyl linkages of sodiated S-003 is Gal*p*NAc-(1→3)-Gal*p*, β-Gal*p*-(1→4)-Glc*p*, and α-Fuc*p*-(1→2)-Gal*p*, which can be easily interpreted from the CID spectra. The observed species of fragment ions and their abundances in the CID spectrum strongly suggest that the sodium ion might be positioned in the vicinity of the Gal*p*-NAc-(1→3)-Gal*p* linkage in the sodiated ion $[M+Na]^+$ of S-003. Although the order of linkage stability in the sodiated ion of S-003 follows the order of hydrolysis rate,[24,25] the order in CID experiments does not always correspond to that of hydrolysis rate (e.g., N-001 in Fig. 1).

The positions of the sodium ion in the $[M+Na]^+$ molecules for all of the oligosaccharides in this paper were examined by interpreting their CID spectra similar to

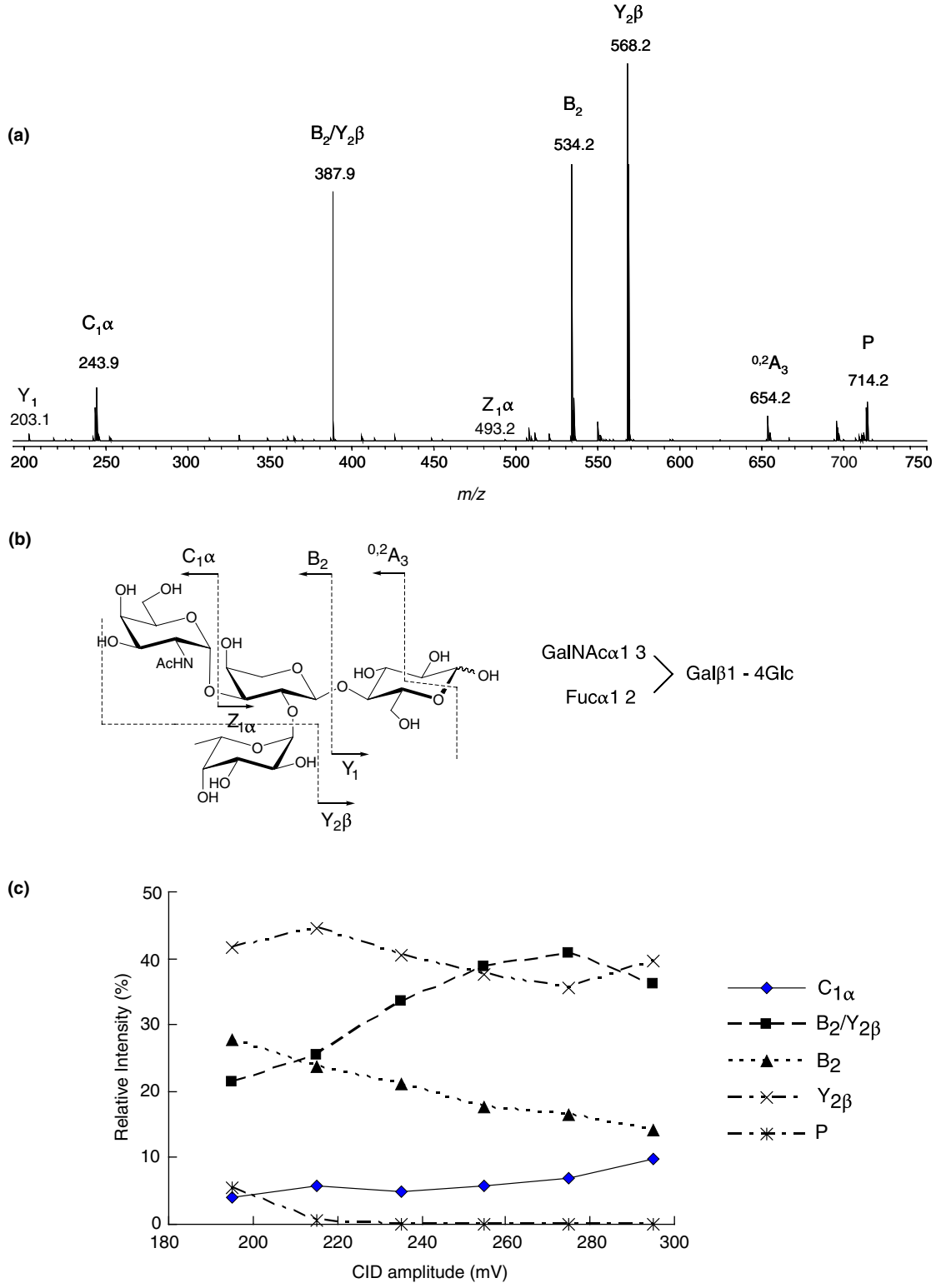

Figure 2. (a) MS/MS spectrum of $[M+Na]^+$ of oligosaccharide S-003. All fragment ions were observed as sodium-adduct ions. P: parent ion. All other symbols for fragment ions are shown in (b). (b) The structures of the fragment ions of S-003. (c) CID energy dependence of the relative intensities for all major fragment ions of S-003. The error bars for the points are estimated at ±3%.

the process described for S-003. The experimentally assigned MS/MS fragment ions for the 27 oligosaccharides using QIT-TOF MS are listed in Figure 1. The low-energy CID process is most likely responsible for cleaving the single glycosic linkages to yield the B/Y and C/Z-series fragmentation products. The assigned

peaks (B/Y and C/Z-series) are listed for the five most abundant fragment ions in the order of their relative intensities.

3.2. Calculation of the sodium ion stabilities

Figure 3 shows six possible structures of Na-adduct complexes for $[A\text{-}034+Na]^+$, which has 92 atoms and 270 vibrational degrees of freedom. The Na^+ affinities of the ions for A-034 ($A\text{-}034+Na^+ \rightarrow [A\text{-}034+Na]^+$) calculated at the PM5, HF/6-31G(d), and B3LYP/6-31G(d)/6-31G(d,p) level are listed in Table 1. The results of the PM5 calculations in terms of the order of stability of the complexes were consistent with the ab initio calculations using the HF and B3LYP methods. Figure 4a shows the computed structure of the most stable $[A\text{-}034+Na]^+$ complex. The calculations indicate that the energy for the structure of $[A\text{-}034a+Na]^+$, in which the sodium ion interacts with the amide oxygen of the Glc*p*NAc residue in Figure 4a, is about 13 kcal/mol more stable than the second stable structure in Figure 3b. The complex shows a tetradentate interaction between the metal ion and the carbonyl oxygen (O2N) of Glc*p*NAc, the hydroxyl oxygen (O6) of Gal*p*, the hydroxyl oxygen (O2) of Fuc*p*, and the glycosyl oxygen between Glc*p*NAc and Fuc*p*. The calculated structure

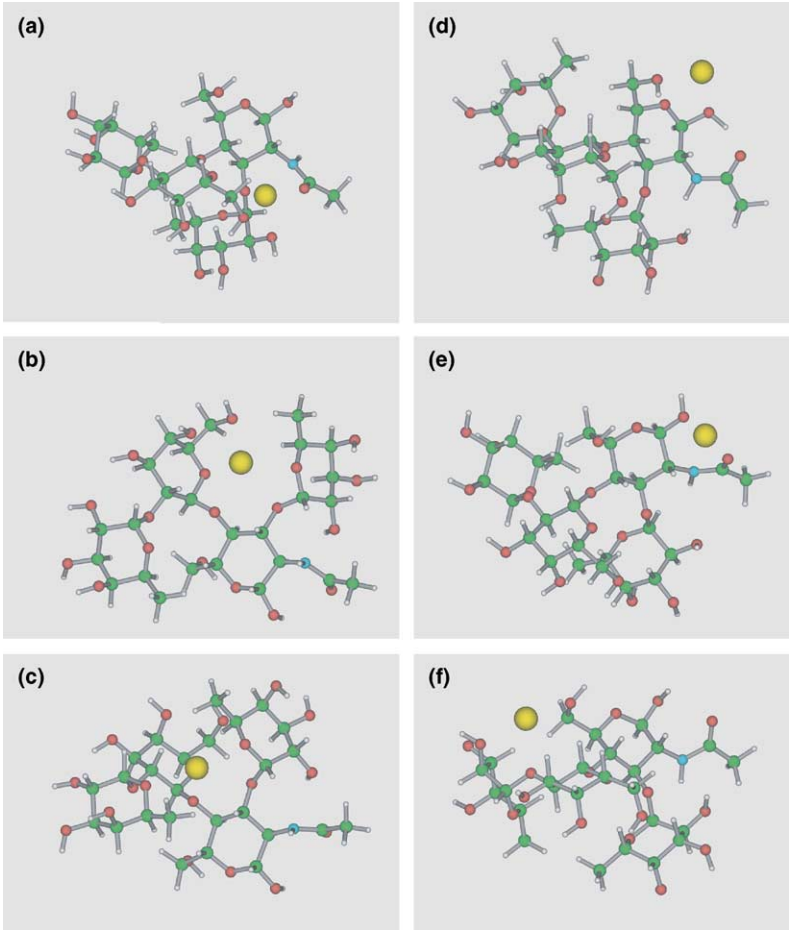

Figure 3. PM5 optimized geometries of the stable conformers of $[(A\text{-}034)+Na]^+$.

Table 1. Na ion binding affinity[a]

	PM5	HF/6-31G(d)	B3LYP/6-31G(d)	B3LYP/6-31+G(d,p)
A-034a	−74.0	−104.4	−106.9	−94.3
A-034b	−61.0	−87.9	−91.6	−79.0
A-034c	−53.8	−77.1	−79.0	−70.3
A-034d	−46.5	−67.1	−72.8	−61.5
A-034e	−44.0	−62.7	−67.3	−57.7
A-034f	−41.7	−61.8	−64.8	−57.5

[a] Units are kcal/mol. The order from the most to least stable structure is from A-034a to A-034f.

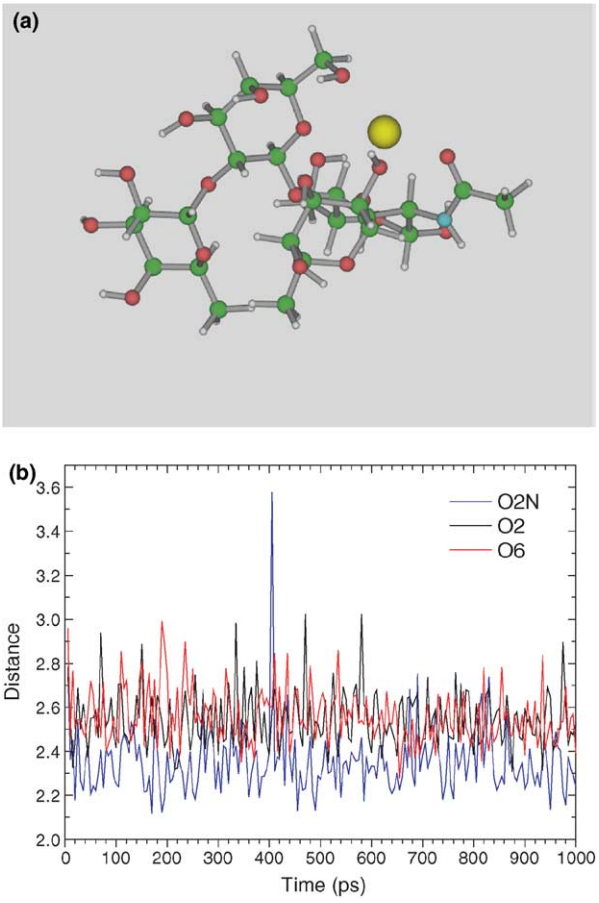

Figure 4. (a) Optimized geometry (PM5) of the most stable conformer of $[A\text{-}034+Na]^+$. Bonding interactions are indicated by the dashed lines, and the corresponding bond lengths are given in angstroms. The distances from the Na^+ ion to the oxygen atoms (O2N, O2, and O6) are 2.27, 2.29, and 2.30 Å, respectively. (b) Distance to the Na^+ ion to the oxygen atoms as a function of time in a constant-temperature molecular dynamics simulation at a temperature of 298 K. The blue, red, and black lines are the distances from the Na atom to the oxygen atoms of O2N, O2, and O6, respectively.

clearly shows that the metal cation is in the vicinity of Glc*p*NAc for the $[A\text{-}034+Na]^+$ complex. To study the stability of this conformation for the complex, a constant-temperature molecular dynamics simulation was performed at a temperature of 298 K.[26] The distances between the Na^+ ion and the oxygen atoms were monitored (Fig. 4b). The distance of the oxygen atoms did not fluctuate much, indicating a stable adduct position for the Na^+ ion in the complex. The position of the sodium metal cation with respect to the amide oxygen of Glc*p*NAc could be a preferential site in the metal binding distribution. To gauge the effect of temperature (total energy) on the preferential position of the adduct, MD simulations were conducted at 350, 400, and 500 K. Varying the amount of available energy appeared to have little effect on the Na^+ position distributions. This indicates that after the sodium cation binds to the oligosaccharide, the conformer exists predominantly as the initial complex structure. In the experimental results, the m/z value for the most abundant fragment ion was observed at 552 Da ($Y_{2\alpha}$), corresponding to the cleavage of the glycosidic bond between Gal*p* and Fuc*p*. The uneven distribution of the Na-adduct position in the $[A\text{-}034a+Na]^+$ complex may lead to the preferential cleavage of the glycosyl bond of α-Fuc*p*-(1→2). The calculated energies of Na ion affinity for the most stable structure of the 27 oligosaccharides using PM5 method are listed in Figure 1.

3.3. Fragmentation analysis

3.3.1. Oligosaccharides with the reducing end of Man*p*. Cancilla et al. have investigated the fragmentation pathways for protonated and alkali-cationized glycosidic bonds.[27] In the mechanism they reported, a proton is localized at the glycosidic oxygen leading to a charge-induced reaction. A similar mechanism was suggested by Hofmeister et al. to explain the bond cleavages in lithium-cationized gentiobiose.[28] On the other hand, it has also been theorized that metal ions interact with several oxygen atoms in oligosaccharides for the stabilization of the glycosidic bond, leading to a remote-charge reaction.[29,30] The activation energy of the protonated oligosaccharides leading to the cleavage of the glycosidic bond that produces the Y/B and C/Z-type fragmentation is smaller than that of the alkali-cationized samples.[31,32] The multiple binding between the cation and the oxygen atoms leads to a highly stable form of the complex ion. The stability may increase with an increasing number of Na^+–oxygen interactions.

The experimental oligosaccharides containing Man*p* as a reducing end were A-031, A-038, and A-039. The cross-ring fragment ions 0,2A and 2,4A, which arise from the reducing termini of *N*-glycans, were observed as the most abundant ion. In these molecules, the dissociation energy for the appearance of cross-ring cleavage ions was determined to be lower than that of the glycosidic cleavages between two Man*p* residues. Figure 5 shows the Na-adduct structures for A-038 and A-039. The calculated preferential adduct position of the Na ion was located on the bisecting branches of these oligosaccharides, which increases not only the number of oxygen atoms that can be accessed by the Na^+ ion, but also those on the reducing termini of Man*p*. The favorable Na-adduct position in Figure 5 makes the glycosidic bonds stronger than those in the neutral case. The experimentally observed major fragment ions are the cross-ring cleavage ions for $[A\text{-}038+Na]^+$ and $[A\text{-}039+Na]^+$ at $m/z = 478$ and 599.3 Da, respectively, which can be assigned to 0,2A and 2,4A, respectively. The calculated results of the Na^+ ion position for A-031, A-038, and A-039 are consistent with the experimentally observed cross-ring cleavages in the charge-remote process.

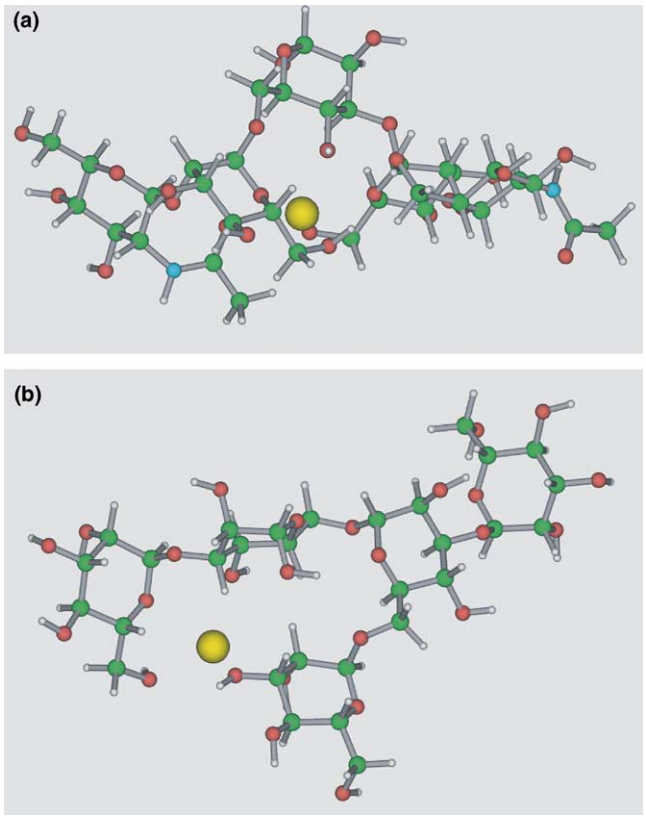

Figure 5. Optimized geometry (PM5) of the most stable conformer of (a) $[A\text{-}038+Na]^+$ and (b) $[A\text{-}039+Na]^+$. The energies of the Na affinity for (a) and (b) are −84.6 and −61.8 kcal/mol, respectively.

3.3.2. Oligosaccharides with Neu*p*5Ac and Fuc*p*. Fuc*p* and Neu*p*5Ac are terminal sugars in oligosaccharides as well as in glycopeptides and glycoproteins. It is known that Neu*p*5Ac and Fuc*p* residues are easily cleaved in low-energy CID,[33] leading to difficulty in the identification of the exact attachment site and the branching location by MS methods. To avoid the loss of sialic acid in the fragmentation reaction under low-energy CID conditions, Powell and Harvey studied the stabilization of the glycosidic bond of Neu*p*5Ac in the analysis of positive ion MALDI MS by converting the sialic acid moieties of Neu*p*5Ac into methyl esters.[33,34]

The experimental oligosaccharides containing Neu*p*5Ac as a terminal nonreducing unit in this study were GSL-003, M-012, A-035, and A-036. In these samples, the highest intensities of the fragment ions corresponding to the loss of 291 Da ($[M+Na]^+$–Neu*p*5Ac) were observed. A-035 and A-036 containing Neu*p*5Ac and Fuc*p* both had intense peaks representing the respective losses of Fuc*p* and Neu*p*5Ac. The results of the observed fragment ions for A-035 and A-036 show a more intense peak associated with the loss of 291 Da ($[M+Na]^+$–Neu*p*5Ac) compared with that of 146 Da ($[M+Na]^+$–Fuc*p*). This indicates that the energy required to cleave the glycosidic bond of Neu*p*5Ac is lower than that of Fuc*p*. A loss of sialic acid appears as the most frequent fragmentation reaction under low-energy CID conditions. Accordingly, the sialylated B and C ions characterizing the terminal epitopes are frequently present in low abundance. Because Neu*p*5Ac has a carboxyl group at carbon atom 1, the sodium cation has a tendency to interact with the oxygen atoms of the carboxyl group, based on both their terminal localization and negative charge (acidic functionality). Proton loss from the carboxyl group of the sialic acid was presumed to occur during the Y cleavage.

To investigate the bond energy of the glycosidic bonds for A-035 that leads to fragmentation into the B/Y ion series, ab initio calculations were performed. In these calculations, the geometry was fully optimized by the HF/6-31+G* method used for zero point energy (ZPE) corrections. The calculated glycosyl bond energies of Glc*p*NAc–Glc*p*, Glc*p*NAc–Fuc*p*, and Neu*p*5Ac–Gal*p* were 60.7, 54.6, and 43.1 kcal/mol, respectively. The energy of the glycosyl bond between Neu*p*5Ac and Glc*p* that produces B/Y type ions is significantly lower than that of the other bonds. The calculated bond energies (Glc*p*NAc–Glc*p* > Glc*p*NAc–Fuc*p* > Neu*p*5Ac–Glc*p*) are directly related to the order of stability in the glycosyl linkage, which correlates to the abundance of the experimentally observed fragment ions in S-003. These calculations suggest that the glycosyl bond cleavage in Neu*p*5Ac oligosaccharides may be less dependent on the position of the alkali metal ion, because the trigger for the cleavage at the glycosidic bond is the migration of the proton from the carboxyl group of the sialic acid on the glycosyl oxygen atom.

In the CID spectra of the oligosaccharides containing Fuc*p* (A-022, A-023, A-024, A-028, A-029S-004, A-033, A-034, S-003,A-040, A-041, M-005, M-006, and M-007), a fucose loss was also observed as the favorable glycosidic cleavage in the fragmentation studies reported here. In our experiments, the dominant product ions were produced from cleavage of the glycosidic bond between Fuc*p* and Gal*p* and were assigned as $Y_{2\beta}$, giving $[S\text{-}003+Na]^+$–Fuc*p* as the highest relative ion abundance (see Fig. 2a and b). The preferential adduct positions of the Na^+ ion for the oligosaccharide $[S\text{-}003+Na]^+$ were investigated to compare the experimentally obtained CID spectra with the calculations (see supplementary data). In the calculations, the most stable structure has a tetradentate interaction between the metal ion with the oxygen atom (O3) of Glc*p*, the hydroxyl oxygen (O6) of Gal*p*, the ring oxygen (RO) of Gal*p*, and the glycosyl oxygen between Glc*p* and Gal*p*. The interaction of the Na^+ ion with the oxygen atoms makes the glycosyl bond between Glc*p* and Gal*p* stronger so that the dissociation energy to cleave the glycosyl bond between Fuc*p* and Gal*p* is the lowest in $[S\text{-}003+Na]^+$.

To explore the fragmentation mechanism of the configuration isomers, we analyzed α,α-, α,β-, and β, β-disaccharide in a D_2O system using collision-induced

dissociation MS/MS measurements in quadrupole/time-of-flight mass spectrometry.[21,28] The results indicate that the fragmentation of the glycosidic bond involves the hydrogen atom of the C-2 hydroxyl group rather than the C-1 and C-2 hydrogen atoms. The proton transferred via this dissociation process comes from the H/D exchangeable hydrogen atoms (–OH hydrogen atoms) rather than the C–H hydrogen atoms, indicating that the hydrogen atom at the C-2 hydroxyl group is involved in the cleavage mechanism of the glycosidic bonds. This fragmentation of the glycosidic bond to form B/Y-type ions may introduce the formation of an epoxide ring (between C-1 and C-2). In the case of Fuc*p* loss, the cleaved Fuc*p* residue forms the epoxide (1, 2-epoxy-hexose). Because Fuc*p* does not have a hydroxyl group on its sixth carbon, the electronegativity of the residue is less than that of the other residues, making Fuc*p* a less favorable site for the binding position of the Na^+ ion.

3.3.3. Oligosaccharides with Glc*p*NAc. The internal fragment ions in Figure 1 were observed for A-033 ($Y_{2\alpha}/Y_{1\alpha}$), A-034 ($Y_{2\alpha}/Y_{1\beta}$), A-038 (Y_2/Y_2), S-003 ($B_2/Y_{1\beta}$), M-006 ($B_2/Y_{1\alpha}$), and M-007 ($B_2/Y_{1\beta}$). These oligosaccharides contain either Glc*p*NAc and Fuc*p* residues (A-033, A-034, S-003, M-006, M-007) or Glc*p*NAc and Man*p* residues (A-038), and have branching chains (biantennary and triantennary structures). In the case of the complexes that have two Fuc*p* units ($[A\text{-}033+Na]^+$ and $[A\text{-}034+Na]^+$), the primary internal fragment ion is due to the loss of the Fuc*p* units ($Y_{2\alpha}/Y_{1\alpha}$). The calculated stable structure of $[M\text{-}007+Na]^+$ involved the Na^+ ion interacting with the oxygen atoms of Fuc*p*, Gal*p*, and Glc*p*NAc. The Na cation in the complexes was in the vicinity of Gal*p*NAc. In addition, C type fragmentation was observed in S-003, M-005, M-006, and M-007, which have Glc*p*NAc and Fuc*p* units in the single and bisecting chains. In the cases of the sample (e.g., A-035 and A-036) containing Glc*p*NAc, Fuc*p*, and Neu*p*5Ac residues, the loss of Neu*p*5Ac was only observed as the fragment ion. For samples like M-005 in which there is no branching in the sugar chain, there was no internal fragment ion observed.

4. Conclusions

Theoretical calculations were performed for sodiated oligosaccharides and compared with the experimental studies to obtain more information about the structure–reactivity relationship of fragmentation reactions in mass spectrometry. Several computational methods, such as molecular dynamics (MD) simulations, semi-empirical (PM5), and electron orbital (HF and B3LYP) calculations, were used to interpret and analyze the experimentally observed fragmentation ions of oligosaccharides using a QIT-TOF mass spectrometer. The ab inito (HF and B3LYP) calculations indicated trends in the binding interaction energies that suggested that the PM5 calculation is adequate in studying the affinity energy. Using the PM5 method, the Na-adduct position in the oligosaccharides was investigated to establish the relationship between the sodiated structures and the resulting ions. The Na-adduct position was explored for the oligosaccharides containing Neu*p*5Ac and Fuc*p*, or Man*p* as a reducing end, or Glc*p*NAc. The Na position was less crucial in terms of the resulting fragment ions from the loss of Fuc*p* and Neu*p*5Ac because of the acidic functionality and electronegativity of the Neu*p*5Ac and Fuc*p* residues. The calculated structures for the oligosaccharides containing Man*p* as a reducing end and Glc*p*NAc indicated an increase in stability with an increasing number of oxygen atoms interacting with the Na^+ ion. The highly stabile complexes exhibited this multiple interaction factor and linkage flexibility. The preferential Na-adduct position in the calculations was in the vicinity of GlcNAc, which was consistent with the experimental results.

In our calculations, the stability of many different conformations was studied in an attempt to establish the dependence of the stability of the complex on the sodium-adduct position. It was difficult to determine a single initial conformation for oligosaccharides with more than five monosaccharide units due to the high conformational flexibility. Recently, molecular dynamics simulations employing principle coordinate analysis (PCA) have been used to establish several dominant conformations for oligosaccharides having more than 5 residues.[35] By sampling these initial configurations, the interaction of the metal ions (Li, Na, and K) and the oligo/polysaccharides are calculated to investigate the structures containing metal ions with the experimentally observed fragment ions.

Acknowledgments

This work was supported by The New Energy and Industrial Technology Development Organization (NEDO) as a part of The Research and Development Projects of Industrial Science and Technology Frontier Program in Japan.

Supplementary data

Supplementary data associated with this article can be found, in the online version, at doi:10.1016/j.carres.2006.01.013.

References

1. Dwek, R. A.; Butters, T. D. *Chem. Rev.* **2002**, *102*, 283–284.

2. Kameyama, A.; Kaneda, Y.; Yamanaka, H.; Yoshimine, H.; Narimatsu, H.; Shinohara, Y. *Anal. Chem.* **2004**, *76*, 4537–4542.
3. Zaia, J. *Mass Spectrom. Rev.* **2004**, *23*, 161–227.
4. Park, Y. M.; Lebrilla, C. B. *Mass Spectrom. Rev.* **2005**, *24*, 232–264.
5. Ojima, N.; Masuda, K.; Tanaka, K.; Nishimura, O. *J. Mass Spectrom.* **2005**, *40*, 380–388.
6. Kameyama, A.; Kikuchi, N.; Nakaya, S.; Ito, H.; Sato, T.; Shikanai, T.; Takahashi, Y.; Takahashi, T.; Narimatsu, H. *Anal. Chem.* **2005**, *77*, 4719–4725.
7. Kikuchi, N.; Kameyama, A.; Nakaya, S.; Ito, H.; Sato, T.; Shikanai, T.; Takahashi, Y.; Narimatsu, H. *Bioinformatics* **2005**, *21*, 1717–1718.
8. Kameyama, A.; Kikuchi, N.; Nakaya, S.; Ito, H.; Sato, T.; Shikanai, T.; Takahashi, Y.; Narimatsu, H. *Glycobiology* **2004**, *14*, 1069.
9. Cancilla, M. T.; Wong, A. W.; Voss, L. R.; Lebrilla, C. B. *Anal. Chem.* **1999**, *71*, 3206–3218.
10. Franz, A. H.; Lebrilla, C. B. *J. Am. Chem. Soc.* **2002**, *13*, 325–337.
11. Sekiya, S.; Yamaguchi, Y.; Kato, K.; Tanaka, K. *Rapid Commun. Mass Spectrom.* **2005**, *19*, 3607–3611.
12. Perreault, H.; Costello, C. E. *J. Mass Spectrom.* **1999**, *34*, 184–197.
13. http://www.cachesoftware.com/mopac/index.shtml.
14. Pankiewicza, R.; Pawowsk, A.; Schroedera, G.; Przybylskia, P.; Brzezinski, B.; Bartl, F. *J. Mol. Struct.* **2004**, *694*, 155–163.
15. Allen, F. H. *Acta Crystallogr., Sect. B* **2002**, *58*, 380–388.
16. Allen, F. H.; Motherwell, W. D. S. *Acta Crystallogr., Sect. B* **2002**, *58*, 407–422.
17. Taylor, R. *Acta Crystallogr., Sect. D* **2002**, *58*, 879–888.
18. Ponder, J. W.; Richard, F. M. *J. Comput. Chem.* **1987**, *8*, 1016–1024.
19. Ren, P.; Ponder, J. W. *J. Comput. Chem.* **2002**, *23*, 1497–1506.
20. Ren, P.; Ponder, J. W. *J. Phys. Chem. B* **2003**, *107*, 5933–5947.
21. Fukui, K.; Takahashi, K.; Akiyama, Y.; Yamagaki, T. *Abstr. Papers Am. Chem. Soc. 074-CARB Part1* **2004**, *228*, U230.
22. Woods, R. J.; Dwek, R. A.; Edge, C. J.; Fraser-Reid, B. *J. Phys. Chem. A* **1995**, *99*, 3832–3846.
23. Woods, R. J. *Glycoconjugate J.* **1998**, *15*, 209–216.
24. Lee, B. S.; Krisnanchettiar, S.; Lateef, S. S.; Lateef, N. S.; Gupta, S. *Carbohydr. Res.* **2005**, *340*, 1859–1865.
25. BeMiller, J. N. *Adv. Carbohydr. Chem.* **1967**, *22*, 25–108.
26. Fukui, K.; Naito, Y.; Akiyama, Y.; Takahashi, K. *Eur. J. Mass Spectrom.* **2004**, *10*, 639–647.
27. Cancilla, M. T.; Penn, S. G.; Lebrilla, C. B. *Anal. Chem.* **1998**, *70*, 663–672.
28. Hofmeister, G. E.; Zhou, Z.; Leary, J. A. *J. Am. Chem. Soc.* **1991**, *113*, 5964–5970.
29. Lemonine, J.; Fournet, B.; Despeyroux, D.; Jennings, K. R.; Rosenberg, R.; Hoffmann, E. D. *J. Am. Soc. Mass Spectrom.* **1993**, *4*, 197–203.
30. Zhou, Z. R.; Ogden, S.; Leary, J. A. *J. Org. Chem.* **1990**, *55*, 5444–5446.
31. Cerda, B. A.; Wesdemiotis, C. *Int. J. Mass Spectrom.* **1999**, *189*, 189–204.
32. Yamagaki, T.; Fukui, K.; Tachibana, K. *Anal. Chem.*, in press.
33. Powell, A. K.; Harvey, D. J. *Rapid Commun. Mass Spectrom.* **1966**, *10*, 1027–1032.
34. Hunnam, V.; Harvey, D. J.; Priestman, D. A.; Bateman, R. H.; Bordoli, R. S.; Tyldesley, R. *J. Am. Soc. Mass Spectrom.* **2001**, *12*, 1220–1225.
35. Fukui, K.; Kameyama, A.; Akiyama, Y.; Takahashi, K.; Narimatsu, H., in preparation.
36. Domon, B.; Costello, C. E. *Glycoconjugate J.* **1988**, *5*, 397–409.